Frost flower chemical composition during growth and its implications for aerosol production and bromine activation

Laura Alvarez-Aviles, William R. Simpson, Thomas A. Douglas, Matthew Sturm, Donald Perovich, Florent Domine

Frost flower chemical composition during growth and its implications for aerosol production and bromine activation

Laura Alvarez-Aviles,[1] William R. Simpson,[1] Thomas A. Douglas,[2] Matthew Sturm,[2] Donald Perovich,[3] and Florent Domine[4]

[1] Frost flowers have been proposed to be the major source of sea-salt aerosol to the atmosphere during polar winter and a source of reactive bromine during polar springtime. However little is known about their bulk chemical composition or microstructure, two important factors that may affect their ability to produce aerosols and provide chemically reactive surfaces for exchange with the atmosphere. Therefore, we chemically analyzed 28 samples of frost flowers and parts of frost flowers collected from sea ice off of northern Alaska. Our results support the proposed mechanism for frost flower growth that suggests water vapor deposition forms an ice skeleton that wicks brine present on newly grown sea ice. We measured a high variability in sulfate enrichment factors (with respect to chloride) in frost flowers and seawater from the vicinity of freezing sea ice. The variability in sulfate indicates that mirabilite precipitation ($Na_2SO_4 \cdot 10\ H_2O$) occurs during frost flower growth. Brine wicked up by frost flowers is typically sulfate depleted, in agreement with the theory that frost flowers are related to sulfate-depleted aerosol observed in Antarctica. The bromide enrichment factors we measured in frost flowers are within error of seawater composition, constraining the direct reactive losses of bromide from frost flowers. We combined the chemical composition measurements with temperature observations to create a conceptual model of possible scenarios for frost flower microstructure development.

1. Introduction

[2] Frost flowers are vapor-deposited ice crystals that wick brine from the sea ice surface and thus they contain high bulk salinities. Early studies of frost flowers focused on their physical properties and the sea ice environment where they form [*Drinkwater and Crocker*, 1988; *Perovich and Richter-Menge*, 1994]. Laboratory experiments investigated the temperature dependence of frost flower growth and the infrared emission of frost flowers [*Martin et al.*, 1995, 1996]. Frost flowers may be responsible for a significant fraction of the salt aerosol available during winter and spring in polar regions [*Rankin et al.*, 2000,

2002; *Rankin and Wolff*, 2003], and have also been proposed to be a source of reactive bromine to the Polar lower atmosphere [*Rankin et al.*, 2002; *Kaleschke et al.*, 2004; *Jones et al.*, 2006]. However, because of difficulties in locating and collecting frost flowers, only a few studies have observed their chemical composition, and often with small sample numbers [*Rankin et al.*, 2000, 2002; *Simpson et al.*, 2005; *Douglas et al.*, 2005; *Kalnajs and Avallone*, 2006].

1.1. Impacts of Frost Flowers on Atmospheric Chemistry

[3] Because of their formation in the polar regions and their potential for mediating exchange between the atmosphere and sea ice surface, frost flowers may play a major role in the tropospheric chemistry of polar regions during the winter. It is widely established that aerosol particles provide sites for heterogeneous chemistry and at the same time, they transport with the wind, dispersing chemical constituents far from their original source [*Wagenbach et al.*, 1998; *Ianniello et al.*, 2002; *Rankin and Wolff*, 2003]. Possible sea-salt aerosol sources include ocean spray, blowing of snow containing sea salts, and frost flowers [*Domine et al.*, 2004]. Aerosol particle generation from frost flowers,

---

[1]Geophysical Institute and Department of Chemistry and Biochemistry, University of Alaska Fairbanks, Fairbanks, Alaska, USA.

[2]US Army Cold Regions Research and Engineering Laboratory, Fort Wainwright, Alaska, USA.

[3]US Army Cold Regions Research and Engineering Laboratory, Hanover, New Hampshire, USA.

[4]Laboratoire de Glaciologie et Géophysique de l'Environnement, CNRS and Université Joseph Fourier-Grenoble, Saint Martin d'Heres, France.
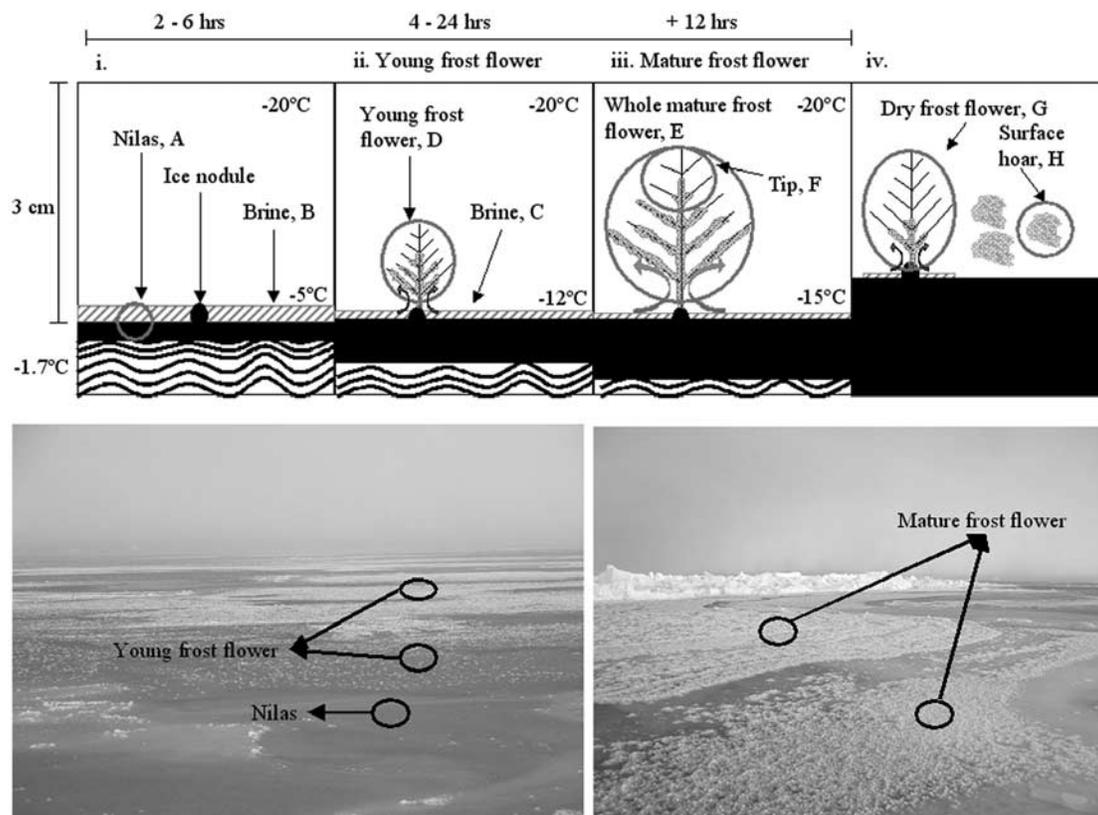
Figure 1. A conceptual model of frost flower growth. The first three panels represent life stages of frost flower growth: (i) Nilas and ice nodules, (ii) Young frost flowers, and (iii) Mature frost flowers. Panel (iv) represents different environments that are physically close to or related to the frost flower growth process, like "dry" frost flowers (that is, frost flowers that do not have as much brine available to wick) and surface hoar. These types are predominantly comprised of water vapor condensed as ice. The circles represent the types of samples collected from the field. All black lines and black shaded areas indicate ice and blue lines or blue shaded or gray shaded areas are brine or snow. The photographs at the bottom illustrate different frost flower growth environments.

or the brine that surrounds them, could explain events of high salt loading in winter months, when young sea ice (nilas) replaces open water near coastal sampling sites [*Rankin et al.*, 2000]. In a year-long study of size segregated aerosol compositions at Halley, Antarctica, *Rankin and Wolff* [2003] estimated that at least 60% of the total sea salt arriving at Halley is from brine and frost flowers on the sea ice surface rather than from sea spray sourced from open water. The primary evidence that brine and/or frost flowers are a source of sea-salt aerosol is that aerosol SO_4^{2-} is depleted with respect to Cl^- in comparison to seawater [*Rankin et al.*, 2000, 2002]. In this paper, we concentrate on the chemical composition of frost flowers, brine, and seawater, and we use these measurements to make constraints on the role of frost flowers in aerosol particle formation.

[4] Chemical models indicate that gas-phase bromine forms when Br^- present in ice reacts with HOBr to release Br_2 that is in turn photolyzed to produce bromine atoms [*Fan and Jacob*, 1992; *Tang and McConnell*, 1996; *McConnell et al.*, 1992; *von Glasow and Crutzen*, 2007; *Simpson et al.*, 2007a]. Frost flowers could promote Br^- activation if HOBr reacted with Br^- in frost flowers. Or,

frost flowers could release aerosols containing Br^- that react with HOBr. Bromine monoxide, BrO, forms from the reaction of gas-phase bromine atoms and ozone. The catalytic reactions of bromine atoms and BrO result in episodes of almost total destruction of tropospheric ozone [*Barrie et al.*, 1988]. The origin and formation of BrO-enriched air masses during tropospheric ozone destruction events are not yet fully understood. Satellite observations of BrO spatially match air masses rich in BrO with potential frost flower (PFF) formation sites [*Kaleschke et al.*, 2004]. However ground-based observations of BrO at Barrow, Alaska find no correlation between BrO and potential frost flowers, but show good correlation between BrO and first year sea ice contact [*Simpson et al.*, 2007b]. In this paper, we present observations of bromide in frost flowers to consider their possible role in halogen activation.

1.2. Frost Flower Growth Process

[5] Figure 1 shows a model of the frost flower growth process. This figure was made by combining our field observations from three years of field campaigns on the sea ice north of Barrow, Alaska with proposed mechanisms of frost flower growth [*Perovich and Richter-Menge*, 1994;

Rankin et al., 2002]. The age stages of formation, keyed to the panels in Figure 1, are (i) growth of small (0.5 cm) nodules (ice bumps, as described in *Perovich and Richter-Menge* [1994]) on the nilas (newly formed sea ice, a few cm thick) surface, (ii) growth of young frost flowers on the nodules, and (iii) further growth and cooling into mature frost flowers. Panel (iv) represents other ice crystals that are common where frost flowers grow or are found in close proximity, as described later. Brine, cryo-concentrated salt solutions, is present on the surface of the nilas because the salts are rejected from the freezing ice lattice. Most brine sinks, but some is forced to the surface [*Richardson*, 1976]. Wicking of brine is indicated in Figure 1 by arrows in the upward position from brine on the sea ice surface toward the frost flower ice-skeleton, in panel (ii) and (iii).

[6] The large temperature gradient between seawater ($\sim-1.7°C$) and ambient air above the water surface ($\sim-20°C$ in these cases) leads to water vapor supersaturation with respect to ice [*Andreas et al.*, 2002]. The supersaturated vapor in the air condenses as ice onto the nodules. The source of water vapor at the warm brine/ice surface and rapid growth on a limited number of nucleation points on the surface leads to Mullins–Sekerka growth instabilities [*Mullins and Sekerka*, 1963], explaining the dendritic crystal shapes. Over the course of a few hours, the sea ice grows thicker and the ice surface temperature drops, causing two things to occur: first, brine on the sea ice surface is drawn up onto the frost flower by surface tension, raising their bulk salinity. Second, the brine cools and salts begin to precipitate based on the temperature at which they exceed saturation; however slow nucleation dynamics may allow for some degree of supersaturation on short timescales.

[7] When the supersaturated salts nucleate, these precipitation processes modify the chemical composition of the frost flowers and residual brine. At $-8°C$ Na^+ and SO_4^{2-} are thermodynamically predicted to precipitate as mirabilite ($Na_2SO_4 \cdot 10\ H_2O$). Hydrohalite (NaCl·2 H_2O) does not crystallize from the brine until temperatures are below $-22°C$. Magnesium (Mg^{2+}) and potassium (K^+) do not precipitate until below $-34°C$, as $MgCl_2 \cdot 6\ H_2O$ and $KCl \cdot 6\ H_2O$. However it is important to remember that there is a large temperature gradient in the vicinity of frost flowers, so the flowers themselves are typically warmer than the overlying air. *Martin et al.* [1996] observed that frost flower tips are $4-6°C$ warmer than the air temperature, and their IR emission temperature is $12-16°C$ warmer than the air temperatures, depending upon actual conditions. Therefore, although the air temperature often may go below the $-22°C$ threshold for hydrohalite precipitation, it is less common that frost flowers growing on thin ice cool to temperatures where hydrohalite and Mg^{2+} and K^+ precipitate.

[8] The main purpose of this paper is to propose a conceptual model of the chemical fractionation processes that occur during frost flower growth. We present results from chemical analyses of frost flowers and their components at various life stages of their growth to support our conceptual model. We also consider the chemical composition of frost flowers and their possible role in bromine activation and aerosol production in the lower troposphere.

2. Methods

2.1. Sample Collection

[9] We collected frost flowers near Barrow Alaska, from an active open lead (71.43°N, 156.47°W) located approximately 3 km from Point Barrow during springtime, on 25 March and 1 April 2005. Some of the samples were collected from newly formed ice by the edge of the lead, some were collected from a floating slab that came close to the ice edge. Other samples were collected in the same lead from a boat, and include nilas and very young frost flowers. Air temperatures were stable at around $-22°C$ during both of these sampling events. Ages or growth stages of frost flowers were estimated in reference to the growth scheme described in the introduction. Sea water was sampled at this time and in later years by submerging a polypropylene sampling vial in water either near the sea ice edge or through a hole chopped through the ice. All samples were transported and stored frozen and away from light until analysis about 5 months later. Samples were collected facing into the wind following clean protocols with powder-free gloves and Tyvek suits. To collect frost flower tips, we used tweezers and for brine on sea ice we used a cleaned glass eyedropper. When sampling whole frost flowers, we collected them with the edge of the polypropylene sampling vial. All sampling vials and tools were cleaned in the laboratory using 18.2 $M\Omega$ cm water and were transported to the site packed in 1-gallon Ziploc bags.

2.2. Analytical Procedures

[10] We weighed the sampling vials, 50 mL polypropylene centrifuge tubes, prior to sampling, and after melting the sample to obtain the mass of the sample. The samples were then diluted by adding ultrapure water until the conductivity of the sample indicated it was in the proper analytical range. The volume of ultrapure water added divided by the mass of the frost flower sample constituted a dilution factor that was later used to back-calculate the samples' total salinity. Major anions (F^-, Cl^-, Br^-, SO_4^{2-}, and NO_3^-) were measured using an Ion Chromatograph (Dionex ICS-2000), using a Dionex AS17 separation column. Standards were made using analytical grade reagents with ion ratios designed to mimic the sample matrix and were verified by commercial standards (Dionex).

[11] We use enrichment factors (*Ef*) to compare the ionic concentration ratios we measured in our samples to the values in standard seawater from *Quimby-Hunt and Turekian* [1983]. For example, the enrichment factor with respect to chloride for a given ion, X, is defined by:

$$Ef(X) = \frac{\left(\frac{[X]}{[Cl^-]}\right)_{sample}}{\left(\frac{[X]}{[Cl^-]}\right)_{Seawater}}. \qquad (1)$$

[12] Here, *Ef* (X) is the ion enrichment factor, [X] is the ion concentration in moles per liter, and [Cl^-] is the chloride concentration in moles per liter. Chloride is chosen as the reference instead of the more traditional Na^+ for a number of reasons. First, Cl^- is analyzed in the same chromatograph as the other anions; so fewer possible error sources enter into the measurement. Second, Na^+ is partially removed when

Table 1. Sea-Ice Processed Seawater Br^- and SO_4^{2-} Enrichment Factors (Ef), and Salinity Values[a]

Site	Ef (Br^-)	Ef (SO_4^{2-})	Salinity (‰)	N
Lead edge (2005)	1.00 (±0.04)	2.11 (±0.08)	15.3 (±0.7)	9
Hole on sea ice (2007)	1.00 (±0.03)	1.40 (±0.05)	17.7 (±0.6)	23
Hole on sea ice (2007)	1.06 (±0.01)	1.02 (±0.01)	25.7 (±0.2)	3
Hole on sea ice (2007)	0.95	1.00	35.6	1
Hole on sea ice (2007)	1.01	1.02	27.4	1
Hole on sea ice (2007)	1.01	1.01	27.5	1
Hole on sea ice (2004)	1.09	0.93	32.6	1

[a]In the case of replicate analysis, the value in the parenthesis is the standard deviation. For samples that have more than 1 analyses of the same sample (N), we report the average of the enrichment factors.

mirabilite precipitates thus making it a poorer reference than Cl^-, which is not removed until hydrohalite precipitates at temperatures below −22C. Third, for aerosol or snow samples, addition or removal of Cl^- by atmospheric processes make it a poorer tracer than Na^+ (which does not undergo volatilization reactions). However mass-balance considerations, discussed further below, indicate that frost flowers contain orders of magnitude more Cl^- than can be affected by relatively weaker atmospheric chlorine fluxes. Therefore, Cl^- is an appropriate tracer of sea-salt content in these samples. We also performed analysis using either Na^+ or Mg^{2+} as the sea salt tracer and find completely consistent results but slightly poorer measurement precision and small systematic deviations consistent with mirabilite depletion in the case of using Na^+ as the sea-salt tracer.

[13] A statistical analysis was performed to quantify uncertainties in the measured enrichment factors. We find that the relative standard deviation (RSD = standard deviation/mean) of the analyzed enrichment factors for bromide is 0.02, and for sulfate is 0.07, which was mostly due to variability between differing IC analysis days with less variability on individual days. These RSD values correspond to precisions of the analysis of enrichment factors for each ion.

[14] We use the chloride concentration to calculate the total salt mass fraction, or bulk salinity, and to compare the salt content in the samples. The bulk salinity is calculated from the Cl^- measurement via:

$$S = \frac{[Cl^-] \times DF \times MW_{Cl}}{MF(Cl)_{Seawater}}. \quad (2)$$

[15] In this equation, S is the salinity (g salt per g of frost flower), $[Cl^-]$ is the Cl^- concentration (moles per liter), DF is the dilution factor (liters of diluted solution per gram of frost flowers), MW_{Cl} is the molecular mass of Cl^- (35.453 g/mol), and $MF(Cl^-)_{Seawater}$ is the mass fraction of Cl^- in standard sea water (0.553 g(Cl^-)/g(sea salt) [*Quimby-Hunt and Turekian*, 1983]). This calculation yields the bulk salinity as a mass fraction in grams of salt per gram of frost flower, and is multiplied by 1000 to present the results in parts per thousand by weight (‰). We note that precipitation reactions modify the composition of the brine, for instance, complete removal and separation of mirabilite would remove ∼10% of the salt mass. However none of our samples are completely sulfate depleted, indicating that this effect causes <10% error in calculation of bulk salinity from Cl^- abundance.

3. Results

[16] The enrichment factors (Ef) for Br^- and SO_4^{2-} and the calculated salinity values of sea ice processed seawater

samples are shown in Table 1. The term "sea ice processed seawater" refers to ocean water that has been in contact with forming and melting sea ice. There are seven samples of sea ice processed seawater: one from 2004, from a hole cut in the sea ice; one from 2005, from the lead edge and five from 2007, from holes on the sea ice. Table 2 shows enrichment factors for Br^- and SO_4^{2-} and the calculated salinity values of frost flowers and their components. The sample letters in Table 2 correspond to the letters and circles in Figure 1. There are 28 samples of different types of frost flower components: six samples correspond to forming sea ice or brine, six are young frost flowers, 10 are mature frost flowers, two are tips of mature frost flowers, two are dry frost flowers, and two are surface hoar.

3.1. Sea Ice Processed Seawater

[17] In this study, enrichment factors and salinity values are calculated with respect to standard seawater, equation (1). We collected seawater samples on the sea ice from different sites with the original purpose of quality assurance of our ion chromatographic analyses. However, through replicate

Table 2. Salinity Values, SO_4^{2-} and Br^- Enrichment Factors in Frost Flowers, Brine and Surface Hoar in Different Life Stages of Frost Flower Growth

Sample	Description	Salinity (‰)	Ef (Br^-)	Ef (SO_4^{2-})
A	Nilas (ice and surface brine)	16	0.98	1.03
		23	0.98	1.03
B	Brine on 1 cm thick nilas	38	0.96	1.01
		35	0.96	1.02
C	Brine on moving slab	80	0.96	1.04
		69	0.97	1.05
D	Young whole frost flower	96	0.98	0.88
		91	0.98	0.96
		87	0.97	1.05
		49	0.97	1.08
		46	0.97	1.08
		81	0.98	1.12
E	Mature whole frost flower	107	0.98	0.35
		85	0.98	0.35
		106	0.98	0.82
		16	0.96	0.92
		22	0.96	0.92
		94	0.97	0.94
		94	0.98	0.97
		20	0.96	0.98
		24	0.96	0.99
		58	0.98	1.43
F	Mature frost flower tip	17	0.97	0.78
		14	0.97	0.89
G	Mature dry whole frost flower	26	0.97	0.8
		16	0.98	0.91
H	Surface hoar	2	0.30	0.66
		2	0.56	0.66

analyses of these samples, we find that some are significantly different from standard seawater (see Table 1). We found that salinity in the sea ice processed seawater samples is variable and below that of standard sea water, with a range of more than a factor of two. This effect is expected because of sea ice freezing dynamics, which separates ice from brine. Brine that is more concentrated than the underlying sea water sinks, which may leave a fresher sample if both sea water and small or melted ice crystals are sampled. The $Ef(Br^-)$ is close to unity (standard seawater ratio) while $Ef(SO_4^{2-})$ shows enrichment at low salinity values and approaches unity as the salinity increases toward that of Arctic Ocean seawater, which is typically around 32‰. Samples that originate from holes in the sea ice seem to have higher salinity values while the ones from the lead edge have the lowest salinity values and the greatest SO_4^{2-} enrichment. After observing that our sea ice processed seawater samples show enrichment factors different from that of standard seawater we called these samples sea ice processed seawater to make a clear distinction from standard sea water.

3.2. Bulk Salinity of Frost Flowers

[18] Bulk salinity of the samples in the frost-flower environment range from 16‰ for nilas to 107‰ for mature whole frost flowers. The high variability in bulk salinity where frost flowers form has been previously reported [*Perovich and Richter-Menge*, 1994; *Rankin et al.*, 2000] and is attributable to the thermodynamics of sea ice and frost flower formation processes. As sea ice freezes, the new ice, nilas, contains nearly pure ice and brine channels that contain concentrated brine, some of which drains out of the ice, decreasing the bulk salinity, as observed in our nilas samples (type A in Table 2 and referring to the type from Figure 1). The brine fractionated to the surface is concentrated with respect to ocean water, and as the ice thickens and brine channels constrict (removing water), one would expect the sea ice surface brine salinity to increase. This effect is exhibited by our salinity measurements, where the brine salinity on 1 cm thick nilas (type B), is ∼36‰, and increases as the ice ages and thickens to ∼4 cm thick nilas, where the brine (type C) salinity averages ∼75‰. Frost flower samples are generally, but not always, enriched in bulk salinity as compared to ocean water. For young frost flowers, all samples are more saline than seawater with an average bulk salinity of ∼75‰. Bulk salinity of mature frost flowers (type E) range from 16 to 105‰, and the average is 62‰, which is comparable to our young frost flower samples. The mature frost flower tips (type F) show lower bulk salinity, ∼16‰, than standard seawater. These bulk salinity measurements show that the tips possess more vapor deposited ice and/or less brine than whole mature frost flowers (type E). Dry frost flower samples, which appear dry because they have wicked less brine, (type G) show low bulk salinity values, 16 and 25‰, compared to standard ocean water. The surface hoar samples (type H) have the lowest salinity values, 2‰. As opposed to frost flowers, surface hoar crystals have no brine source from underlying sea ice, and their salinity may be a result of incorporation of sea-salt aerosols, sea spray, or atmospheric gases (for example, H_2SO_4 or HCl) during their growth.

3.3. Sulfate Enrichment Factor of Frost Flowers

[19] Temperature changes and nucleation dynamics at different frost flower growth stages dictate if precipitation processes are to occur. Fairly young (1 to 2 hours old) samples that have not yet cooled below −8C (temperature at the sampling point—for example, the nilas) likely do not contain mirabilite crystals and would be expected to have enrichment factors near unity. Sample types A−C all show this behavior, with the SO_4^{2-} enrichment factor range in nilas and brine comparable to unity. Because the brine and mirabilite crystals probably wick differently up frost flowers, we expect that the sulfate enrichment factor will show variability, and in fact there is a high variability of $Ef(SO_4^{2-})$ between different types of frost flowers and even for the same types. Of the six young frost flower samples (type D),. four have a small enrichment and the other two have a small depletion. Nine of ten mature frost flower samples (type E) are depleted in sulfate, with two depleted down to $Ef(SO_4^{2-}) = 0.35$. The two mature flower tip samples show moderate depletion, $Ef(SO_4^{2-}) = 0.89$ and 0.78. The two dry frost flower samples (type G) show moderate depletion with $Ef(SO_4^{2-}) = 0.91$ and 0.80. The surface hoar samples are depleted, with both samples showing $Ef(SO_4^{2-}) = 0.66$.

3.4. Bromide Enrichment Factor of Frost Flowers

[20] The Br^- enrichment factors for all the frost flower components we collected range from 0.96 to 0.98 while the two surface hoar samples yield values of 0.30 and 0.56. According to our statistical analysis for Br^-, the RSD of the $Ef(Br^-)$ has a 1-σ precision of 0.02 (this includes day-to-day variability). Thus it is evident that the $Ef(Br^-)$ does not vary among any of the components that make up frost flowers or among young or old frost flowers. This findings stands in contrast to the high variability of $Ef(SO_4^{2-})$ we measured. Although there appears to be a slight depletion of ∼3% in all samples, this apparent depletion is not variable and is not dependent on the sample age. Therefore, we expect that analytical uncertainties in the instrument calibration account for this small deviation from unity. Taken in total, our analysis shows that none of the brine-sourced frost flowers or related samples are significantly depleted in Br^-. The surface hoar samples are the only samples that show a considerable depletion in Br^-. Variability of Br^- in snow and a lack of depletion or enrichment in frost flowers has been previously reported [*Simpson et al.*, 2005], although they reported the results from only a few frost flower samples.

4. Discussion

[21] Physical and chemical processes involved in frost flower growth govern where salts are stored on the frost flower ice crystals. In the following sections, we discuss sulfate and bromide enrichment factors and their implication in aerosol formation and bromine activation in the atmosphere and synthesize the results from our detailed chemical analysis into a conceptual model of frost flower growth and microstructure.

4.1. Sea Ice Processed Seawater

[22] Frost flowers and brine on the sea ice surface form from seawater that is available; therefore at early stages of
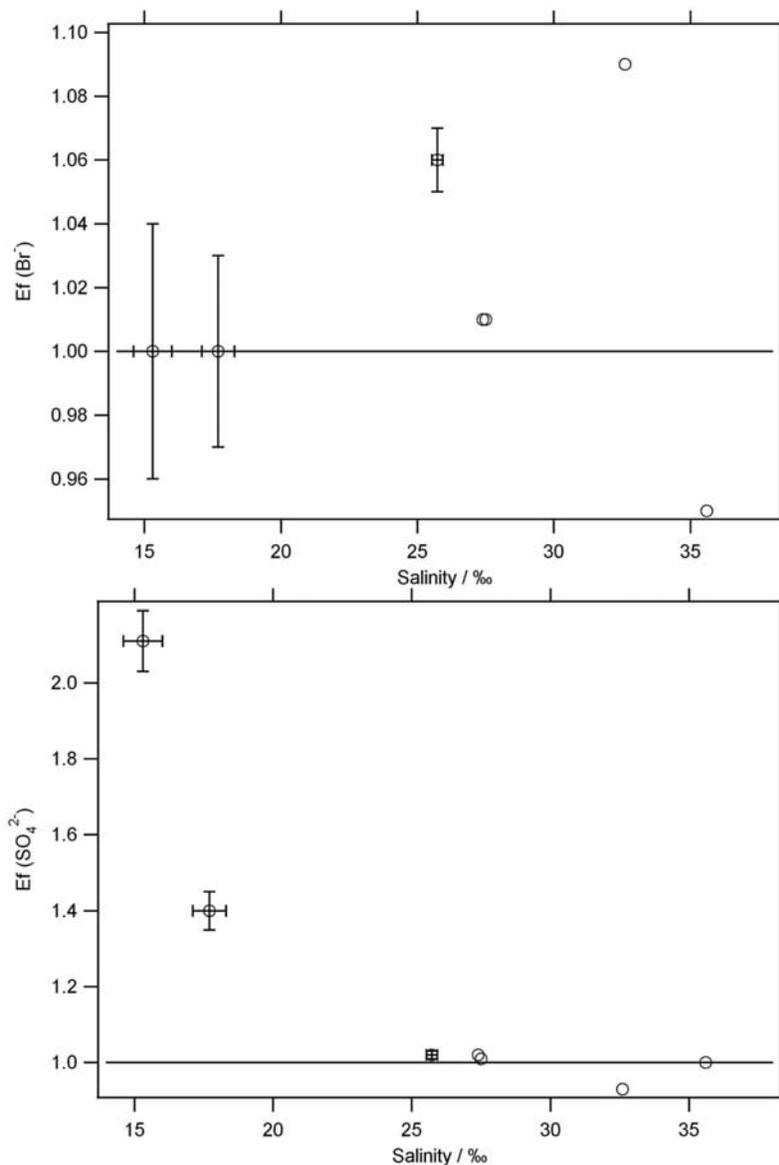
Figure 2. Bromide and SO_4^{2-} enrichment factors as a function of Arctic seawater salinity (in parts per thousand, ‰).

frost flower growth they mostly reflect the chemical composition of the seawater from which they originated. Some of our sea ice processed seawater samples, particularly ones characterized by low salinity, show $Ef(SO_4^{2-})$ different than standard seawater. Figure 2 shows $Ef(Br^-)$ and $Ef(SO_4^{2-})$ versus salinity for the sea ice processed seawater samples. Figure 2 reinforces what Table 1 summarizes: $Ef(Br^-)$ is close to unity with no apparent trend in salinity, and $Ef(SO_4^{2-})$ shows greater enrichment at low salinity and is comparable to standard seawater as salinity increases. On the basis of what is presented in Figure 3 the SO_4^{2-} enrichment in low salinity samples could be attributable to mixing mirabilite precipitate on the surface of young sea ice with seawater. As mirabilite crystallizes on the sea ice surface and the sea ice cracks, the mirabilite crystals can mix with seawater that is being diluted by the incorporation of melting broken sea ice or forming crystals (frazil ice) [*Comiso et al.*, 2003]. Adding mirabilite to

seawater adds SO_4^{2-}, thereby increasing $Ef(SO_4^{2-})$. If the water is fresher than standard seawater, it would float on top of the denser sea water, and would have been measured by our surface water sample. If this sulfate-enriched sea ice processed seawater were to be involved in new nilas formation that formed frost flowers, there could be some degree of SO_4^{2-} enrichment in the initially formed nilas and frost flowers.

4.2. Salinity of Frost Flowers

[23] The bulk salinity of frost flowers provides important constraints on their growth mechanism and resulting microstructure. Our salinity findings are similar to what was previously reported by *Perovich and Richter-Menge* [1994] who found that as the temperature of the environment in which the frost flowers form decreases, the bulk salinity of the frost flowers increases. Our observation that the tips of frost flowers are of lower bulk salinity than the frost flowers
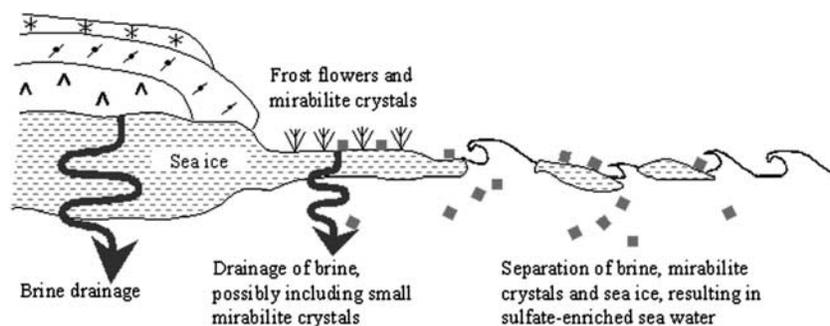
Figure 3. A schematic diagram of sea-ice processed seawater formation. The left portion of the figure shows frost flowers on nilas in the presence of mirabilite precipitate (squares), and sea salt migration downward through channels in the sea ice (arrows). As mirabilite forms, the fractionated brine is separated from the mirabilite precipitate. The separation of fractionated brine and mirabilite precipitate occurs when the fractionated brine migrates or drains away from the nilas area. The right portion of the figure shows an opening on the sea ice where surface brine drains into the ocean. If this sample contains mirabilite, and ice, they will melt when in contact with warmer seawater, resulting in less saline, sulfate-enriched sea-ice processed seawater that will float on the denser normal seawater.

as a whole is in agreement with the idea that the dendritic tips of frost flowers grow by rapid vapor condensation or that brine has not yet wicked to this point. *Domine et al.* [2005] observed that the morphology of frost flower tips was consistent with rapid vapor deposition. These observations indicate that frost flowers grow largely by vapor deposition of ice to form a ''skeleton'' that defines the overall macroscopic morphology followed by brine wicking that provides salts. Temperature affects frost flower skeletal morphology, as noted in *Martin et al.* [1996]. Other evidence that the skeleton formation is not related to the presence of brine is that frost flowers grow on freshwater ice [*Domine et al.*, 2005; *Gosnell*, 2005].

[24] The frost flowers become saline by wicking brine from the young sea ice surface. The bulk salinity of frost flowers ($\sim$50–100‰) and the ambient temperatures of the environment in which they form (approximately −10°C, at the frost flowers base) locate frost flowers in a two-phase region of the phase diagram for sea ice [*Weeks and Ackley*, 1982]. The composition and temperature indicate roughly equal parts of ice and brine. For this reason, we present the conceptual picture of the frost flower macrostructure shown in Figure 4, left panel.
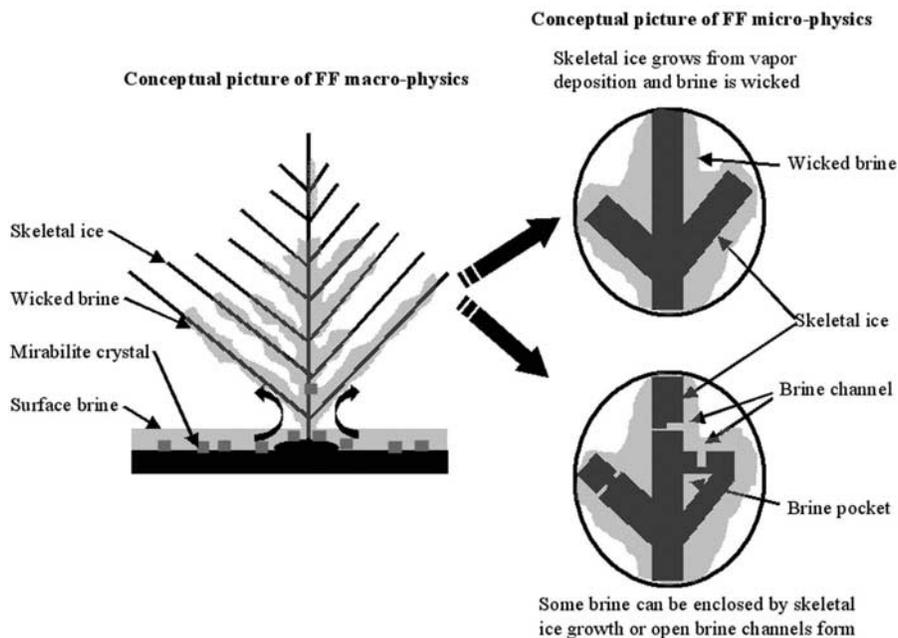
[25] The microstructure of frost flowers is not well defined by the bulk measurements presented here, but we can identify two limiting cases, as shown in the right panel of Figure 4. In the first case, brine is assumed to be present only on the outside of an ice skeleton, and in the second case, brine inclusions or channels also form in the ice lattice. The photomicrographs presented in *Domine et al.* [2005] appear to show that at least some brine is present on the surface and rounds the angular forms of the vapor-deposited ice skeleton. As frost flowers cool, the sea ice phase diagram [*Weeks and Ackley*, 1982] shows that the brine becomes more concentrated as water molecules add to existing ice or form new ice. Depending on the morphology of the frost flower ice skeleton and the availability of brine, all or some of the frost flower surface area is likely to be wetted by brine. The composition of brine is a function of temperature, as predicted by the phase diagram, and not a function of the bulk salinity.

Higher bulk salinity simply indicates a higher fraction of brine than ice. Therefore, if we consider a hypothetical frost flower fully wetted by brine, its surface composition is that of the brine, while measuring its bulk composition will yield the proportion of skeletal ice to wicked brine. On the other hand, if freezing brine within frost flowers leads to the growth of inclusions or channels, included brine may not be available on the frost flower surface. Formation of channels could cause pressurization and pumping of brine could occur, as it does when bulk sea ice freezes. The microstructural details of this process are unclear at this point and should be further studied.

4.3. Sulfate in Frost Flowers

[26] The sea ice phase diagram is useful when considering the chemical composition of frost flowers. Unfortunately, the thermodynamics expressed in the phase diagram are most useful for closed systems, and frost flowers, sea ice, and all of the samples considered here are not closed systems because we only collected parts of the complete system. Specifically, liquid brine is more mobile than ice or precipitates thus brine wicking is likely to be associated with salts that have a different composition than seawater once precipitation occurs. Sea ice samples show salinity deviations from seawater (ice–salt separation), but as long as they are warmer than −8°C, no mirabilite precipitation should occur. Therefore, nilas and sea ice surface brine at early stages should have SO_4^{2-} enrichment factors near their seawater source, in agreement with the observations of types A to C (Table 2 and Figure 1). As time advances and the temperature decreases below −8°C, mirabilite precipitation should become thermodynamically favorable. Some spatial regions within the frost flowers/ice-surface brine/sea ice environment where mirabilite precipitation occurs could contain more (or less) mirabilite crystals than others and thus be enriched (or depleted) in SO_4^{2-}. Therefore, we interpret the variability in $Ef(SO_4^{2-})$ as evidence that our samples are from the spatial location of mirabilite precipitation and separation of mirabilite from SO_4^{2-} depleted brine.

[27] Mirabilite is denser than brine (1.46 vs. about 1.08 g cm^{-3}, [*Porter and Spiller*, 1956; *Dougherty*, 2001])

Conceptual picture of FF macro-physics

Conceptual picture of FF micro-physics

Skeletal ice grows from vapor
deposition and brine is wicked

Wicked brine

Skeletal ice

Skeletal ice

Wicked brine

Mirabilite crystal

Surface brine

Brine channel

Brine pocket

Some brine can be enclosed by skeletal
ice growth or open brine channels form

Figure 4. A conceptual model of possible macro- and micro-structures involved in frost flower growth and the related chemical separation. The tips of the frost flowers are shown as not yet wetted by brine and they are primarily vapor-deposited "skeletal ice". The ice surface is covered with brine that cools and precipitates mirabilite crystals, leading to wicked brine that is depleted in sulfate. The ice-sea salt phase diagram indicates that frost flowers are two or more phase systems (ice, brine, and precipitate), but the microstructure of the ice is unknown. Skeletal ice may grow as the brine cools (right top), or ice may overgrow brine forming pockets and channels (right bottom).

so its crystals would sink and are expected to be less likely to be wicked up along with brines colder than $-8°C$. However the fall velocity of a spherical 1 μm diameter mirabilite crystal [*Light et al.*, 2003] through brine would be about 0.2 mm per hour (derived by application of the Stokes Law assuming a brine viscosity of 0.003 Pa s, which corresponds to 100‰ salinity) so that sedimentation may be too slow to lead to fractionation in all cases. Likewise, mirabilite may fail to nucleate even when it is supersaturated, so that SO_4^{2-} depletion would not always be observed, especially for young frost flowers. This slow rate of sedimentation is consistent with the observation that aged frost flowers are more depleted in SO_4^{2-} than younger frost flowers.

[28] Our observations of SO_4^{2-} fractionation in frost flowers helps develop a conceptual model of frost flower growth and chemical fractionation, shown in Figure 4. Mirabilite crystals (squares) are precipitated mostly in the sea ice surface brine, and the brine that is wicked by the frost flower is SO_4^{2-} depleted. We can generally characterize our observations of SO_4^{2-} fractionation in the samples into classes of warmer samples, which are unfractionated or slightly enriched SO_4^{2-} and older, colder samples (for example, older frost flowers or tips), which generally exhibit SO_4^{2-} depletion.

[29] Sea ice processed seawater can be a source of SO_4^{2-} enriched nilas and brine that is wicked by frost flowers. Enrichment in mature frost flowers is less likely to occur according to our observations, so our one highly enriched mature frost flower could be explained in multiple ways. First, while collecting the mature frost flowers it is possible that we accidentally sampled mirabilite from the brine at the

base of the frost flowers. This brine contains mirabilite precipitate crystals that when added to the SO_4^{2-} depleted frost flower could result in SO_4^{2-} enrichment. We mentioned previously that as time advances, brine on the sea ice surface diminishes but mirabilite precipitate crystals left behind may be more available, and therefore, easier to collect. Second, as mirabilite precipitation occurs on the frost flower, external processes can remove the liquid brine leaving behind attached to the frost flower the mirabilite precipitate resulting in enhancement. External processes that remove liquid brine from the frost flower could include brine droplets being blown away from the frost flower, or the mechanical breakage of frost flower parts that have depleted brine around it. And third, if the brine from which the frost flowers originate is SO_4^{2-} enriched because of sea ice processed seawater, these frost flowers should show enrichment in SO_4^{2-}. Fourth, enrichment of sulfate could result from attachment of non-sea-salt sulfate (for example, Arctic haze-derived sulfate); however *Toom-Sauntry and Barrie* [2002] indicate that atmospheric addition to fresh snow typically adds on the order of 10 μM sulfate, which is undetectably small as compared to sea-salt sulfate in these samples (1,000–80,000 μM).

[30] Frost flowers are believed to be a major source of sea salt aerosol [*Rankin et al.*, 2000, 2002; *Rankin and Wolff*, 2003], but the mechanism by which frost flowers produce aerosol particles is not well established. *Rankin and Wolff* [2003] propose mechanical breakage of frost flowers as the aerosol source. However our sampling of frost flowers shows that they are fairly mechanically rigid and appear difficult to fracture or break, at least on the macroscopic

scale. This macroscopic rigidity was also observed by *Domine et al.* [2005]. Drying of frost flowers could increase their fragility and allow production of salt fragments. Another possible aerosol particle formation mechanism would be for brine to blow from the frost flower structure, producing aerosol directly from the brine. An even more extreme mechanism might be if brine channels form, as discussed in section 4.3, pressurization of the channel could produce brine that might produce aerosol particles. If inclusions form, their partial freezing during the cooling of the frost flower would probably lead to ice/brine particle production, in a manner similar to the rime-splintering mechanism of *Hallett and Mossop* [1974] that was proposed to explain the formation of large numbers of ice particles in clouds.

[31] It is useful to use the aerosol observations to consider the size of brine or frost flower fragments that would be needed to produce the observed aerosol particles. *Rankin and Wolff* [2003] reported that winter sea-salt aerosol particle diameters measured in Antarctica commonly range from 0.2 to 2 μm. To produce a dry salt aerosol particle of this size, the diameter of a 75‰ brine droplet is approximately 4 times larger than a dry aerosol particle. Thus 0.2−2 μm salt aerosol particles would be the result of drying brine droplets on the order of 0.8−8 μm. Direct aerosol production by mechanical breakage of frost flowers would require similar sized fragments based upon the bulk composition of the frost flowers; however it is quite likely that there is a great deal of heterogeneity in the chemical composition of frost flowers at the microscopic scale.

4.4. Bromide in Frost Flowers

[32] Depletion of Br$^-$ can occur when Br$^-$ ions have been activated to gas-phase reactive bromine species. Field observations of snow samples have shown a significant number of snow samples are depleted in Br$^-$, which was taken as evidence of production of reactive bromine [*Simpson et al.*, 2005]. Enrichment would result from the addition of Br$^-$ through the termination step of reactive bromine chemistry, reaction of bromine atoms with VOCs, which produces HBr. Addition of Br$^-$ through HBr could explain the enrichment in Br$^-$ reported in aerosols [*Barrie et al.*, 1988; *Ianniello et al.*, 2002], in some snow pack samples [*Simpson et al.*, 2005], and in model simulations [*Sander et al.*, 2006].

[33] We found that only the surface hoar collected close to frost flowers was significantly depleted in Br$^-$, but none of the frost flower samples or brine samples were significantly depleted or enriched in Br$^-$. These observations agree with the idea that salts in the surface hoar are likely to come from the atmosphere, while salts in all of the other samples come from the ocean via sea ice processes. *Douglas et al.* [2008] proposed that surface hoar is an efficient mercury scavenger thus it is likely that surface hoar is also an efficient sea-salt aerosol scavenger. Atmospheric salts are affected by bromine chemistry and aerosol formation mechanisms while the directly ocean-derived salts are primarily affected by precipitation reactions (for example, mirabilite precipitation). The lack of Br$^-$ depletion in frost flowers might imply they do not play a role in Br$^-$ activation chemistry. However a consideration of the bromine mass balance shows that significant atmospheric abundance of

reactive bromine could be produced with small depletions of Br$^-$ from the extremely saline frost flowers. Observed BrO levels near the ground could be as large as 50 pptv during ozone depletion events [*Wagner et al.*, 2001; *Hoenninger and Platt*, 2002]. If we assume 50 pptv of BrO for a 1 km high atmosphere column at −40°C, there are 2×10^{14} molecules/cm^2 of bromine. Frost flower salinities can be more than 100‰, which implies a Br$^-$ concentration of approximately 3×10^{-3} moles per liter. For 1 cm high frost flowers with a density of 0.02 g/cm^3 [*Domine et al.*, 2005] there are 4×10^{16} molecules/cm^2 of Br$^-$. Thus the frost flower column density is 200 times larger than the atmospheric column density value. As a consequence, for a frost flower to satisfy the total atmospheric budget of Br$^-$ there has to be a 0.5% Br$^-$ depletion in frost flowers. This 0.5% depletion is smaller than our measurement precision and thus is not detectable, yet it could significantly affect lower tropospheric halogen chemistry. This simple calculation ignores the fact that many airmasses do not have such a high BrO column density and that frost flowers do not cover the whole region below BrO events and thus should be taken to be only an order-of-magnitude estimate. However it is still clear that frost flowers could release bromine in amounts that significantly affect the atmosphere while only changing *Ef*(Br) by small enough amounts to escape detection (a few percent). Our results constrain the bromine release budget from frost flowers better than any previous measurements and show that it is maximally on the order of atmospheric column abundances.

5. Conclusions

[34] The bulk chemical analysis of numerous frost flowers and related samples presented here reinforces the previously proposed formation mechanism for frost flowers [*Perovich and Richter-Menge*, 1994; *Rankin et al.*, 2002]. In this mechanism, the bulk morphology is determined by vapor deposition of water in a supersaturated environment followed by wicking of brine up the ice skeleton. Consideration of the phase diagram for sea ice indicates that the structure of frost flowers is a multi-phase system with nearly pure ice, cryoconcentrated brine, and precipitate crystals. The brine has a composition controlled by the temperature and the mobility of brine, which allows separation of brine from ice and precipitates. However the microstructure of the frost flowers remains unknown by our studies of bulk composition. This microstructure could be relatively simple, with a brine liquid layer coating an ice skeleton, or much more complex with brine channels or inclusions. The microstructure is critical to understanding chemical reactions on the surface of frost flowers because it controls the surface composition of reactants on the flowers. The observation of high variability in SO$_4^{2-}$ enrichment factors is consistent with the frost flower/ice-surface brine/sea ice environment being the location where mirabilite crystals separate from SO$_4^{2-}$ depleted brine. Typically, younger, warmer samples have sulfate enrichment factors near unity, while older, colder samples appear depleted in sulfate. From this consideration, we support the argument that mirabilite crystals separate from brine that is SO$_4^{2-}$ depleted in this environment and that frost flowers

may produce sulfate depleted aerosol through this mechanism. Clearly, field and laboratory measurements should be directed toward observations of aerosols produced from frost flowers. Bromide enrichment factors are essentially all unity, indicating no fractionation of Br^- in frost flowers, in agreement with previous observations [*Rankin et al.*, 2002; *Simpson et al.*, 2005]. While this observation appears to argue against frost flowers as a source of reactive bromine to the atmosphere, a mass balance shows that frost flowers contain a greater bromine pool than the typical lower atmospheric burden so they could still be a significant bromine source to the atmosphere.

References

Andreas, E. L., P. S. Guest, P. O. G. Persson, C. W. Fairall, T. W. Horst, R. E. Moritz, and S. R. Semmer (2002), Near-surface water vapor over polar sea ice is always near ice saturation, *J. Geophys. Res.*, *107*(C10), 8032, doi:10.1029/2000JC000411.

Barrie, L. A., J. W. Bottenheim, R. C. Schnell, P. J. Crutzen, and R. A. Rasmussen (1988), Ozone destruction and photochemical reactions at polar sunrise in the lower Arctic atmosphere, *Nature*, *334*, 138–141.

Comiso, J. C., J. Yang, S. Honjo, and R. A. Krishfield (2003), Detection of change in the Arctic using satellite and in situ data, *J. Geophys. Res.*, *108*(C12), 3384, doi:10.1029/2002JC001347.

Domine, F., R. Sparapani, A. Ianniello, and H. J. Beine (2004), The origin of sea salt in snow on Arctic sea ice and coastal regions, *Atmos. Chem. Phys.*, *4*, 2259–2271.

Domine, F., A.-S. Taillandier, W. R. Simpson, and K. Severin (2005), Specific surface area, density and microstructure of frost flowers, *Geophys. Res. Lett.*, *32*, L13502, doi:10.1029/2005GL023245.

Dougherty, R. C. (2001), Density of salt solutions: effect of ions on the apparent density of water, *J. Phys. Chem. B*, *105*, 4515–4519.

Douglas, T., M. Sturm, W. Simpson, S. Brooks, S. Lindberg, and D. Perovich (2005), Elevated mercury measured in snow and frost flowers near Arctic sea ice leads, *Geophys. Res. Lett.*, *32*(4), L04502, doi:10.1029/2004GL022132.

Douglas, T., M. Sturm, W. Simpson, S. Brooks, S. Lindberg, and D. Perovich (2008), Influence of snow and ice crystal formation and accumulation on mercury deposition to the Arctic, *Environ. Sci. Technol.*, *42*, 1542–1551.

Drinkwater, M. R., and G. B. Crocker (1988), Modelling changes in the dielectric and scattering properties of young snow-covered sea ice at GHz frequencies, *J. Glaciol.*, *34*(118), 274–282.

Fan, S. M., and D. J. Jacob (1992), Surface ozone depletion in Arctic spring sustained by bromine reactions on aerosols, *Nature*, *359*, 522–524.

Gosnell, M. (2005), *Ice: The Nature, the History, and the Uses of an Astonishing Substance*, Alfred A. Knopf, New York.

Hallett, J., and S. C. Mossop (1974), Production of secondary ice particles during the riming process, *Nature*, *249*, 26–28.

Hoenninger, G., and U. Platt (2002), Observations of BrO and its vertical distribution during surface ozone depletion at Alert, *Atmos. Environ.*, *36*, 2481–2490.

Ianniello, A., H. J. Beine, R. Sparapani, F. Di Bari, I. Allegrini, and J. D. Fuentes (2002), Denuder measurements of gas and aerosol species above Arctic snow surfaces at Alert 2000, *Atmos. Environ.*, *36*, 5299–5309.

Jones, A. E., P. S. Anderson, E. W. Wolff, J. Turner, A. M. Rankin, and S. R. Colwell (2006), A role for newly forming sea ice in springtime polar tropospheric ozone loss? Observational evidence from Halley station, Antarctica, *J. Geophys. Res.*, *111*, D08306, doi:10.1029/2005JD006566.

Kaleschke, L., et al. (2004), Frost flowers on sea ice as a source of sea salt and their influence on tropospheric halogen chemistry, *Geophys. Res. Lett.*, *31*, L16114, doi:10.1029/2004GL020655.

Kalnajs, L. E., and L. M. Avallone (2006), Frost flower influence on springtime boundary-layer ozone depletion events and atmospheric bromine levels, *Geophys. Res. Lett.*, *33*, L10810, doi:10.1029/2006GL025809.

Light, B., G. A. Maykut, and T. C. Grenfell (2003), Effects of temperature on the microstructure of first-year Arctic sea ice, *J. Geophys. Res.*, *108*(C2), 3051, doi:10.1029/2001JC000887.

Martin, S., R. Drucker, and M. Fort (1995), A laboratory study of frost flower growth on the surface of young sea ice, *J. Geophys. Res.*, *100*(C4), 7027–7036.

Martin, S., Y. Yu, and R. Drucker (1996), The temperature dependence of frost flower growth on laboratory sea ice and the effect of the flowers on infrared observations of the surface, *J. Geophys. Res.*, *101*(C5), 12,111–12,125.

McConnell, J. C., G. S. Henderson, L. Barrie, J. Bottenheim, H. Nili, C. H. Langford, and E. M. J. Templeton (1992), Photochemical bromine production implicated in Arctic boundary-layer ozone depletion, *Nature*, *355*, 150–152.

Mullins, W. W., and R. F. Sekerka (1963), Morphological stability of a particle growing by diffusion or heat flow, *J. Appl. Phys.*, *34*, 323–329.

Perovich, D. K., and J. A. Richter-Menge (1994), Surface characteristics of lead ice, *J. Geophys. Res.*, *99*(C8), 16,341–16,350.

Porter, M. W., and R. C. Spiller (1956), *The Barker Index of Crystals: A Method for the Identification of Crystalline Substances*, W. Heffer, Cambridge, U.K.

Quimby-Hunt, M. S., and K. K. Turekian (1983), Distribution of elements in sea water, *Eos Trans. AGU*, *64*(14), 130–132.

Rankin, A. M., and E. W. Wolff (2003), A year-long record of size-segregated aerosol composition at Halley, Antarctica, *J. Geophys. Res.*, *108*(D24), 4775, doi:10.1029/2003JD003993.

Rankin, A. M., V. Auld, and E. W. Wolff (2000), Frost flower as a source of fractionated sea salt aerosol in the polar regions, *Geophys. Res. Lett.*, *27*(21), 3469–3472.

Rankin, A. M., E. W. Wolff, and S. Martin (2002), Frost flowers: Implications for tropospheric chemistry and ice core interpretation, *J. Geophys. Res.*, *107*(D23), 4683, doi:10.1029/2002JD002492.

Richardson, C. (1976), Phase relationship in sea ice as a function of temperature, *J. Glaciol.*, *17*(77), 507–519.

Sander, R., J. Burrows, and L. Kaleschke (2006), Carbonate precipitation in brine—a potential trigger for tropospheric ozone depletion events, *Atmos. Chem. Phys.*, *6*, 4653–4658, www.atmos-chem-phys.net/6/4653/2006/.

Simpson, W. R., L. Alvarez-Aviles, T. A. Douglas, M. Sturm, and F. Domine (2005), Halogen in the coastal snow pack near Barrow Alaska: Evidence for active bromine air-snow chemistry during springtime, *Geophys. Res. Lett.*, *32*, L04811, doi:10.1029/2004GL021748.

Simpson, W. R., et al. (2007a), Halogens and their role in polar boundary-layer ozone depletion, *Atmos. Chem. Phys.*, *7*, 4375–4418.

Simpson, W. R., D. Carlson, G. Hoenninger, T. A. Douglas, M. Sturm, D. K. Perovich, and U. Platt (2007b), The dependence of Arctic tropospheric halogen chemistry on sea ice conditions, *Atmos. Chem. Phys.*, *7*, 621–627.

Tang, T., and J. C. McConnell (1996), Autocatalytic release of bromine from Arctic snow pack during polar sunrise, *Geophys. Res. Lett.*, *23*, 2633–2636.

Toom-Sauntry, D., and L. A. Barrie (2002), Chemical composition of snowfall in the high Arctic: 1990–1994, *Atmos. Env.*, *36*, 2683–2693.

von Glasow, R., and P. J. Crutzen (2007), Tropospheric halogen chemistry, in *The Atmosphere, 4 Treatise on Geochemistry*, edited by H. D. Holland and K. K. Turekian, Elsevier-Pergamon, Oxford, U.K.

Wagenbach, D., F. Ducroz, R. Mulvaney, L. Keck, A. Minikin, M. Legrand, J. S. Hall, and E. W. Wolff (1998), Sea-salt aerosol in coastal Antarctic regions, *J. Geophys. Res.*, *103*(D9), 10,961–10,974.

Wagner, T., C. Leue, M. Wenig, K. Pfeilstcker, and U. Platt (2001), Spatial and temporal distribution of enriched boundary layer BrO concentrations measured by the GOME instrument aboard ERS-2, *J. Geophys. Res.*, *106*(D20), 24,225–24,235.

Weeks, W. F., and S. F. Ackley (1982), The growth, structure, and properties of sea ice, *Open File Rep. Monogr.*, 82-1, 130 pp., CRREL, USA.

————————

L. Alvarez-Aviles and W. R. Simpson, Geophysical Institute and Department of Chemistry and Biochemistry, University of Alaska Fairbanks, 900 Yukon Drive, Room 186, Fairbanks, AK 99775-6160, USA. (ffwrs@uaf.edu)

F. Domine, Laboratoire de Glaciologie et Géophysique de l'Environnement, CNRS and Université Joseph Fourier-Grenoble, BP 96, 54 rue Molière, F-38402 Saint Martin d'Heres, France.

T. A. Douglas and M. Sturm, US Army Cold Regions Research and Engineering Laboratory, P.O. Box 35170, Fort Wainwright, AK 99703-0170, USA.

D. Perovich, US Army Cold Regions Research and Engineering Laboratory, 72 Lyme Road, Hanover, NH 03755, USA.